Biophysical Journal

Supporting Material

Dynamic force spectroscopy on supported lipid bilayers: effect of temperature and sample preparation

Andrea Alessandrini, Heiko M. Seeger, Tommaso Caramaschi, Paolo Facci

Supporting Methods

Before starting each force curve measurement session, the presence of a lipid bilayer homogeneously covering the support was verified by AFM imaging. Figure S1a shows an AFM image of a POPE bilayer covering the mica surface at 34°C. The featureless image doesn't exclude the possibility of the total absence of the bilayer. To completely exclude this last possibility we change the temperature until a phase transition of the bilayer appears. Figure S1b shows the appearance of solid ordered domains at 27°C. This feature definitively establishes the presence of a lipid bilayer on the mica surface. We then set the temperature at the corresponding value used for the measurement and we wait for about 30 min to allow a complete stabilization of the system.

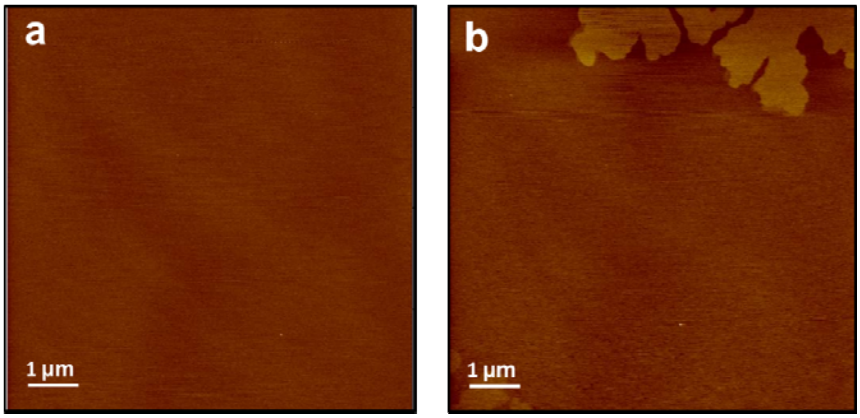

Figure S1: a) AFM image of a POPE bilayer on mica at 34°C in 50 mM KCl pH 7; b) AFM image of the same sample area as in a) at 27°C: the formation of solid ordered domains is evident.

Dynamic force spectroscopy measurements

The dynamic force spectroscopy experiments were performed while keeping constant the time interval between two successive contacts of the tip with the upper surface of the bilayer. This procedure was adopted to avoid artifacts in the experiments coming from the relaxation times of the bilayer after each perturbation by the tip. Hence, each plot in which the most probable punch-through force is reported as a function of the tip speed represents experiments where the only changing parameter is the cantilever vertical speed. Moreover, the sequence of investigated tip speeds was chosen randomly in order to avoid artifacts, such as drifts, in the force values due to tip wearing or solution evaporation. We kept particular attention to acquire the sequence corresponding to the lowest speed as the first one and the sequence corresponding to the second speed (in value) as the last one. Sequences with values coming from the above specified measurements (the first two speed values) not in agreement with the overall trend were discarded. This strategy provides a check for modifications of the tip surface. To balance evaporation and to try to keep as much as possible the ionic strength of the solution at a constant value we maintained constant the volume of liquid in the imaging cell by adding distilled water. It has been demonstrated that an increase of the ionic strength of the solution implies an increase of the punch-through force value. In order to avoid

artifacts coming from evaporation we performed also series of measurements starting from the highest tip speed to the lowest one. In this case the effect of evaporation, if present, should contribute in the opposite direction with respect to the increase of the punch-through force with the increase of the tip speed. The punch-through force from each force curve was obtained by an in-house developed software package.

Force curves and Dynamic Force Spectroscopy on a POPG bilayer with uncoupled leaflets

When force curves are performed on a supported POPG bilayer prepared in order to exhibit uncoupled leaflets, two jump-through events are observed. Figure 1c and 1d in the manuscript show examples of force curves obtained in distilled water and in 50 mM KCl respectively. Figure S2a shows the distribution of the jump-through forces obtained in the same case of figure 1c at a tip speed of 359 nm/s for both the first and the second jump-through event. It is evident that the two distributions are quite separated from each other. If we measure the most probable jump-through force value for the first event as a function of the log(tip speed) we obtain the plot reported in figure S2b. In this case we observe the expected increase in the jump-through force value with the tip speed. The data in figure S2b cannot be fitted by a single linear relation. For the highest explored tip speeds an increase of the dependence of the force on the log(tip speed) is obtained with respect to the lowest speeds. If we prepare the supported POPG bilayer at a temperature higher than the case of figure S2a but still below the conditions required for coupled leaflets and we measure the force curves in 50 mM KCl, the two leaflets will still be uncoupled but the degree of uncoupling should be lower with respect to the case of figure S2a. In figure 1d of the manuscript examples of force curves for two different tip speeds are reported. The degree of coupling between the two leaflets results in the presence of two jump-through events for low tip speeds whereas a single one for higher tip speeds. Figure S2c reports the distributions of the jump-through force values for the two events obtained for the same tip speed as in figure S2a (359 nm/s). As it can be easily seen, the separation between the two distributions is now lower than in case of figure S2a. This difference could be attributed to the different degree of interleaflet coupling. By increasing the tip speed the presence of the two jump-through events changes into the presence of a single event, as shown in the inset to figure S2c, where the distribution of the jump-through force values is shown for a tip speed of 1390 nm/s. Figure S2d shows the dependence of the most probable jump-through force values on the log(tip speed) for the case reported in figure S2c. For the first two tip speeds, where the force curves show the presence of two jump-through events, the value corresponding to the first event is reported.

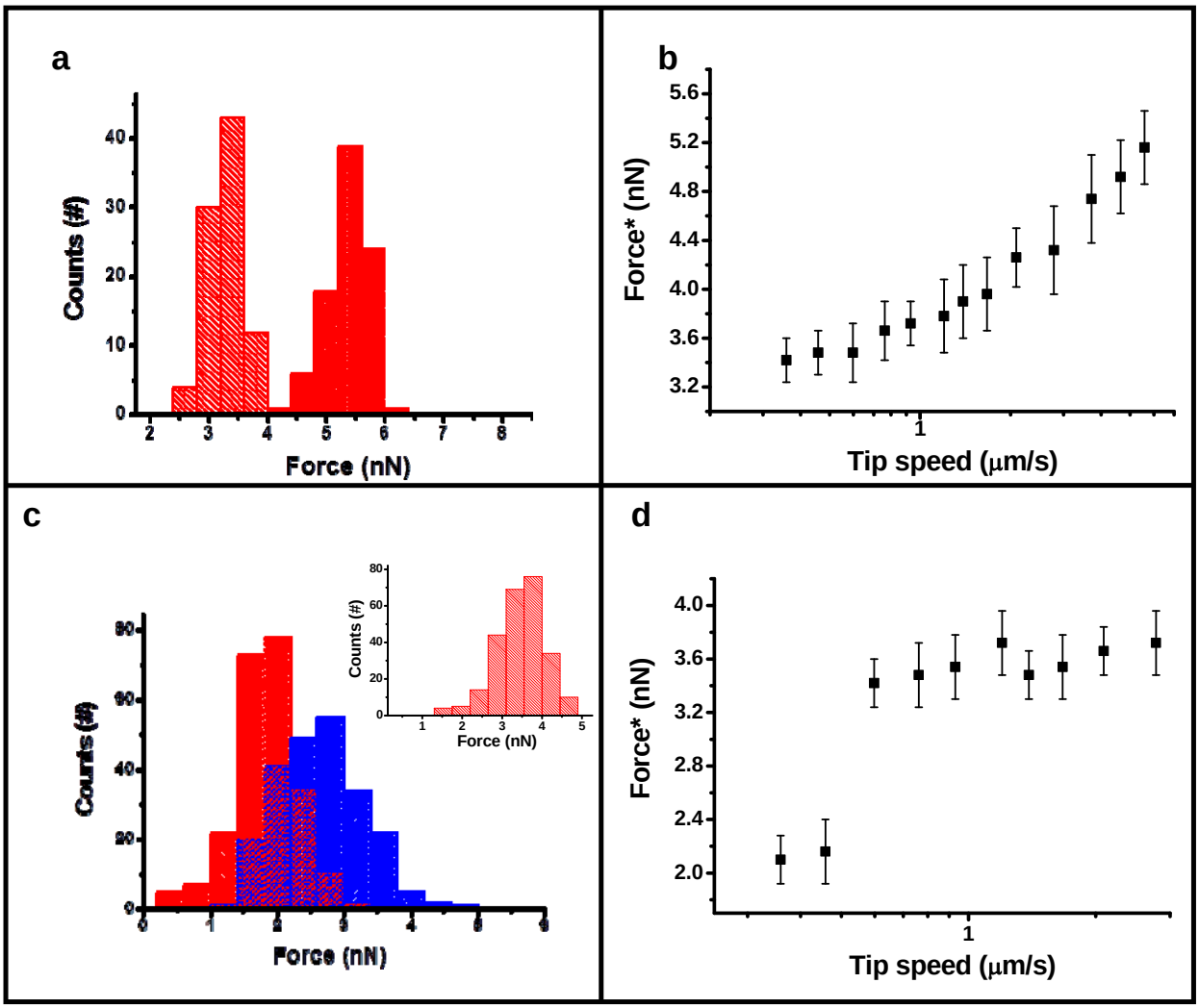

Figure S2: a) Distributions of the jump-through force values for a supported POPG bilayer with uncoupled leaflets. The force curves have been performed with a tip speed of 359 nm/s in distilled water; b) most probable jump-through force for the first event as a function of tip speed for the supported POPG bilayer of a); c) Distributions of the jump-through force values for a supported POPG bilayer with uncoupled leaflets. The force curves have been performed with a tip speed of 359 nm/s in 50 mM KCl. Inset: jump-through force value distribution for the same POPG bilayer performed at a tip speed of 1390 nm/s; d) most probable jump-through force as a function of tip speed for the supported POPG bilayer of c). For the first two speeds which show two penetration events, the force value of the first event is reported.

Figure S3a reports a comparison between two representative force curves obtained on the supported POPG bilayer of figures S2c-d for tip speeds of 359 nm/s (red trace) and 1390 nm/s (black trace). It is evident that the overall jump-through distance is similar in the two cases (one and two penetration events), whereas a difference is observed in the first part of the force curve. It is likely that the higher tip speed produces initially a stronger interdigitation process between the two leaflets increasing their coupling. The increased coupling produces a single penetration event as schematically reported in figure S3b. The proposed description implies that the indentation process by an AFM tip in the direction perpendicular to the plane of the lipid bilayer produces both a vertical and a lateral deformation of the membrane. This hypothesis is consistent with the fact that

the contact region of the force curve on the lipid bilayer measures a combination of the lateral area stretching modulus and the compression modulus. Being the lipid bilayer behavior strongly dependent of the tip speed it is also evident that the overall response is affected by the viscous properties of the involved deformations.

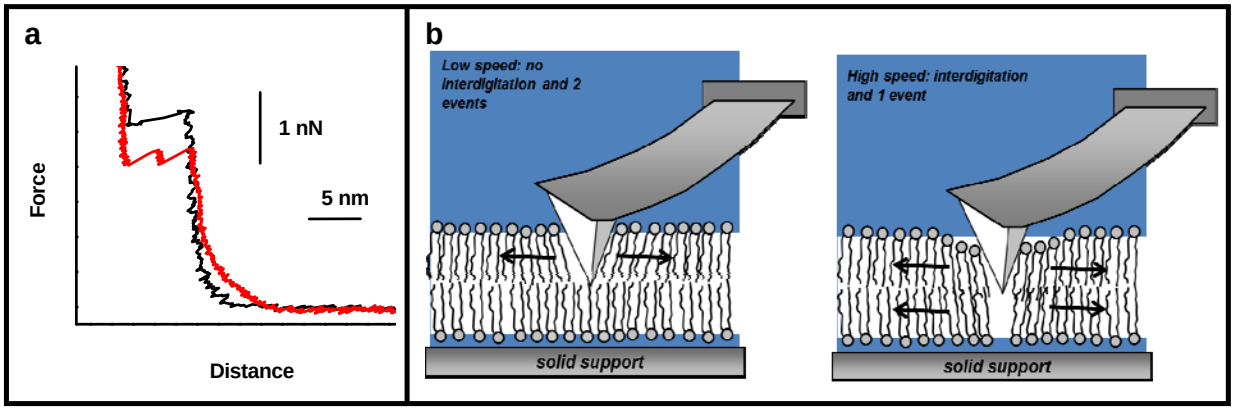

Figure S3: a) Force curves on the supported POPG bilayer of figure S2c. The red trace has been otained at a tip speed of 359 nm/s and the black trace at a tip speed of 1390 nm/s; b) schematics of the penetration process for the AFM tip in the situations of low and high speed. In the low tip speed case the lateral movement of the two leaflets is independent whereas, in the high speed case, due to induced interdigitation by the tip, the two leaflets become coupled and the they move together.

Estimation of the elastic modulus of the supported lipid bilayer

By considering the contact region between the tip and the supported lipid bilayer it is possible to obtain an estimate of the elastic constant of the lipid bilayer. The usually adopted analytical model to analyze indentation experiments by AFM is the Hertz model (or some of its adaptations like the Sneddon one). It has been shown that in the case of supported lipid bilayer the above model is not appropriate. The difficulty mainly stems from the small thickness of the lipid bilayer. In fact, the presence of the rigid substrate under the lipid bilayer could strongly influence the value of the Young modulus obtained by interpreting the stress-strain relation on the basis of the Hertz theory, especially in the case of a high deformation ratio. Here we applied a model developed by Das et al. to extract an estimate for the spring constant of the lipid bilayer [1]. The used model accounts for the presence of the two leaflets composing the bilayer, even if it neglects the strong asymmetry in the physical properties of the two leaflets as due to the presence of the substrate. Apart from the accurate value of the extracted parameters, we are interested in highlighting the variation in the bilayer properties as a function of the different temperatures, especially in the neighborhoods of the phase transition region. The above model is based on the fact that a spherical indenting AFM tip forces the lipids on a curved surface. Accordingly, the area stretching modulus of the lipid bilayer is involved. By calculating the Gibbs free energy cost for the deformation and its derivative with respect to the tip movement they obtain the following analytical expression for the applied force and the bilayer deformation:

$$F = \frac{\pi \kappa_A R}{4}\left(\frac{2 z_0}{2d - z_0}\right)^2 \qquad \text{(S1)}$$

where κ_A is the area stretching modulus, R is the diameter of the apical region of the AFM tip, $2d$ is the thickness of the bilayer on the solid support and z_0 is the indentation in the bilayer. Figure S4 reports a force curve resulting from an average over more than 200 individual force curves obtained on a POPE supported bilayer at 27°C in 50 mM KCl (figure 4 in the manuscript). By fitting the previous equation to the experimental data in the contact region of the force curve (red trace in figure S4) and assuming an apex radius for the tip between 5 nm and 10 nm it is possible to extract a value for κ_A between 0.12 N/m and 0.06 N/m. At 34°C the value for κ_A is between 0.16 N/m and 0.08 N/m whereas at 38°C it is between 0.14 N/m and 0.07 N/m. This analysis shows that AFM force spectroscopy is able to detect the softening effect of the phase transition in the contact region besides the decreased mechanical stability.

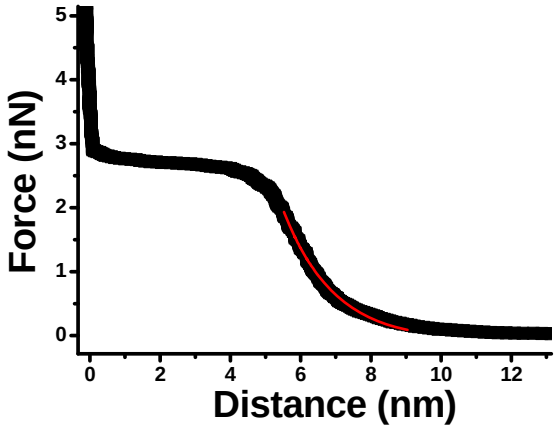

Figure S4: Force curve (resulting from an average over more than 200 individual curves) on a supported POPE bilayer at 27°C in 50 mM KCl (black curve). The red curve is the fit performed with the model of Das et al. to the experimental data.

As it can be seen from figure S4 the fit of the above model to the experimental data is better for high force values than for small values. In this case it is probable that the effect of the compression modulus, which is neglected in the model by Das et al, is more evident in the initial part of the force curve than in the higher force range. We cannot exclude the presence of electrostatic forces due to the fact that measurements were performed in a 50 mM KCl solution which assures a Debye length of about 3-4 nm. However, in this case we were mainly interested in the possibility of comparing the mechanical properties of the bilayer at different temperatures rather than extracting an accurate value for the area stretching modulus. We used a model in which the extracted parameters could be compared to available estimates from other experimental set-ups such as the micropipette aspiration technique. Other models have been developed for atomic force microscopy indentation experiments. Fraxedas et al. [2] developed a model in which the lateral interactions among the constituting elements of the sample play a dominant role and they applied this model also to indentation experiments on lipid bilayers [3]. In another work, Leonenko et al. [4] demonstrated that the Hertz model is not suitable to analyze the deformation of the lipid bilayer induced by the

AFM tip. In fact, nanoscale structural rearrangements are involved in the bilayer compression and steric contributions to the repulsive force are expected [5] giving rise to an exponential dependence of the force on the distance. In a recent paper, Picas et al. [6] extracted from the force curves the Young modulus of the lipid bilayer and then, invoking the thin shell theory, calculated the area stretching modulus and the bending stiffness of the bilayer.

Viscous contributions to force curves

To analyse the possible presence of viscous contributions in the force curves on supported lipid bilayers we compared the force curves obtained at different tip speeds and different temperatures on a POPE bilayer. Each trace reported in figure S5 has been obtained by averaging over 200 individual force curves. The resulting traces have been aligned using the substrate position as reference. It can be noticed that, whereas the force curves acquired at different tip speeds overlap well at 27°C and 38°C, in the case of 34°C they show a significant difference in the contact region. At 34°C the apparent Young modulus of the lipid bilayer increases with the tip speed, pointing to the presence of viscous contributions. At the same time, the force curves at 34°C show that, in the initial contact region between the tip and the bilayer, where probably force components different from the elastic ones are at work, increasing the tip speed causes an increased deformation of the system.

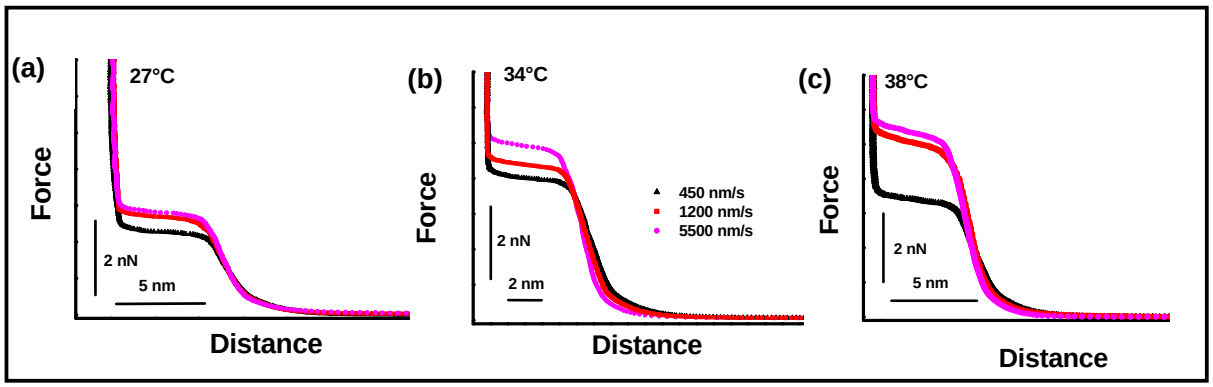

Notably, the initial portion of the contact region, where forces different from a pure mechanical contribution could play a role (for example hydration and electrostatic forces) shows that the higher is the tip speed the more the tip approaches the bilayer. The cause of this sort of shear thinning behavior (decreasing of the viscosity with the increase of the stimulus frequency) is at the moment not understood and it will be further investigated. Considering the plots in figure 3 and the

corresponding analysis of the force curves in figure S5 for the three different temperatures, it seems that a deviation from a linear relation between the most probable jump-through force and the log(tip speed) occurs when the viscous effects are more prominent.

Fit of different models to DFS data

By measuring the jump-through force as a function of the tip speed we observed a behavior reminiscent of dynamic force spectroscopy on, for example, single proteins. In some cases we observed a linear increase of the jump-through force value with the log (tip speed). Accordingly, we decided to use different theoretical models developed for DFS experiments to tentatively extract useful parameters for the process at issue. We applied three available models: the Bell-Evans model, the molecular model proposed by Butt et al. and the Dudko-Hummer-Szabo model. Depending on the adopted model, different parameters can be extracted. The Bell–Evans model allows extracting k_{off}^0 and the distance to the transition state (Δx). k_{off}^0 represents the rate for the event (rupture of a bond or collapse of a lipid bilayer) to occur in the absence of force. For lipid bilayers it is connected to the probability of hole formation in the absence of applied force where the hole is large enough to allow tip penetration. The distance to the transition state expresses the sensitivity of the rate of jump-through to the applied force. A small value of the distance to the transition state means a small sensitivity to the applied force. It must be stressed that the distance to the transition state is extracted on the basis of the assumption of the pulling direction as the reaction coordinate for force spectroscopy experiments. Even if this choice is very intuitive, in some cases it could be a nonrealistic assumption. The phenomenological Bell-Evans model predicts the following relation between the most probable rupture force and the rate of force increase *r*:

$$F^* = \frac{k_B T}{\Delta x}\log r + \frac{k_B T}{\Delta x}\left(\log t_0 - \log\frac{k_B T}{\Delta x}\right) \qquad \text{(S2)}$$

where $t_0 = 1/k_{off}^0$. Figure S6 reports the fit of the Bell-Evans model to the data in the case of POPE at 34°C. Two fits have been performed for the low and high loading rate ranges. From the low tip speed range fit we obtain a figure for Δx of 0.02 nm whereas, for the high tip speed range we obtain a figure of 0.003 nm. For the k_{off}^0 value the two figure of 10^{-7} Hz and 10^2 Hz for the low and high tip speed ranges respectively.

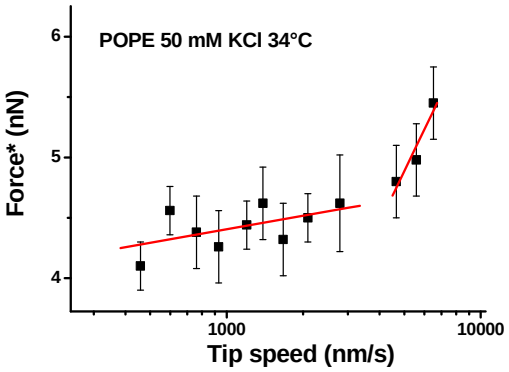

Figure S6: Most probable jump-through force for a suported POPE bilayer with coupled leaflets at 34°C in 50 mM KCl as a function of the tip speed. The low and high tip speed ranges have been fitted by the phenomenological Bell-Evans model

In the phenomenon at issue here the approaching and indenting AFM tip involves not only the compression modulus of the bilayer but also lateral flow phenomena such as shearing of the lipid bilayer and lateral diffusion of lipids. In this context a useful discussion can be made about the k_{off}^0 parameter obtained from the fits of figure S6. The lipid movement which could have characteristic times of interest (not too fast) for dynamic force experiments is the lateral diffusion. All considerations about characteristic times in force spectroscopy experiments on supported lipid bilayers should take into account that the viscosity of the bilayer could be some order of magnitude higher than the corresponding values for unsupported bilayers due to the presence of the substrate. Diffusion coefficients for supported lipid bilayers show that the presence of the substrate usually induces a decreased lateral mobility of the lipids. The characteristic times for lipid lateral movement can affect the rate of spontaneous hole formation (hence k_{off}^0 value) and at the same time they can affect the establishment of viscous effects. Following a similar discussion in a paper by Butt's group [7], we can relate the diffusion constant for lipids to the hopping frequency of lipids between adjacent sites. Diffusion constant for supported lipid bilayers is reported to be in the order of magnitude of a few $\mu m^2/s$. This order of magnitude gives a hopping frequency value much higher than those compatible with the obtained k_{off}^0 (the obtained k_{off}^0 is about 8-10 order of magnitude lower than the hopping frequency for the low tip speed range). However, it must be considered that several lipid molecules are interested at the same time in the jump-through event. Other motions of the lipids such as chain rotation are too fast to be relevant in these experiments. Lipid flip-flop is typically very slow and could be of interest in the present investigation.

The molecular model proposed by Butt allows extracting both the activation energy for the process and k_{off}^0. The data presented in figure S5 can also be fitted with the molecular model developed by Butt. According to this model, the force required for the jump-through event increases linearly with the logarithm of the tip speed as defined by the following equation:

$$F = a + b \ln v \qquad \text{(S3)}$$

where *a* and *b* are parameters which are connected to mechanical properties of the bilayer [8]. Once *a* and *b* are determined by a fit to the data, it is possible to extract the activation energy at zero force. This model doesn't provide the distance to the transition state. Equation S3 clearly foresees a linear relation between the jump-through force and log (tip speed). Accordingly, we separately fitted equation S3 to the two tip speed regions as in figure S6. The fit to the same data of figure S6 of the Butt model produces values for the activation energy of 45 k_BT for the lower range of force increase rate and 31 k_BT for the higher range. However, it is to be stressed that this model assumes that the pre-exponential factor of the Arrhenius dependence equals the resonance frequency of the cantilever.

The last model we fitted to the experimental data on the supported POPE bilayer at 34°C is the DHS one. We performed a fit to the experimental data with the relation describing the value for the average rupture force as a function of tip speed expressed by the following formula:

.

$$\langle F \rangle \cong \frac{\Delta G_\beta}{\nu x_\beta}\left\{1-\left[\frac{k_BT}{\Delta G_\beta}\ln\frac{k_{off}^0 k_BT\exp\left(\frac{\Delta G_\beta}{k_BT}+\gamma\right)}{x_\beta r_F}\right]^\nu\right\}, \qquad \text{(S4)}$$

where γ is a dimensionless constant (its value is *0.577*), ΔG_β is the activation free energy in the absence of applied force, ν is related to the shape of the energy landscape and, in the DHS theory, it can assume the values *1/2* or *2/3* for the cusp and linear-cubic shapes respectively , x_β is the position of the transition state along the reaction coordinate, k_{off}^0 is the force-free reaction rate and r_F the rate of force increase. In figure S7 a fit to the data with $\nu = 2/3$, which represents a quite general free-energy shape for reactions, is reported. It is to be noted that the present model has three fitting parameters instead of two as the previous models. The following parameters result from the fitting procedure: $\Delta G_\beta = 9 k_BT$, $x_\beta = 0.01$ *nm* and $k_{off}^0 = 10^{-12}\ s^{-1}$.

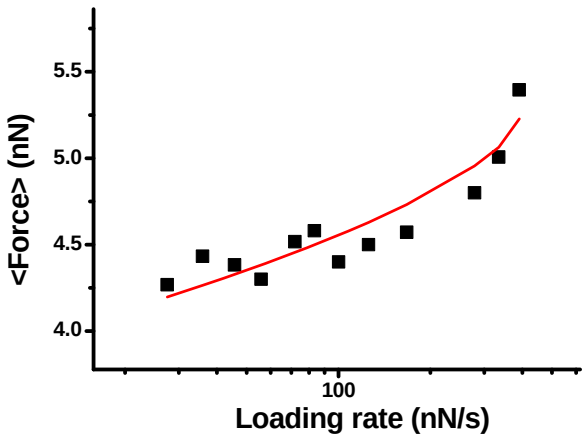

Figure S7: Average jump-through force for a supported POPE bilayer with coupled leaflets at 34°C in 50 mM KCl as a function of the loading rate. The data have been fitted by the DHS model.

The value for the distance to transition state gives a figure of 0.01 nm in the DHS model and similar values (0.02 nm and 0.001 nm for the low and high tip speed range respectively) in the Bell-Evans phenomenological model. It should be pointed out here that, in a previous work by Abdulreda and Moy [9] in which an event involving the fusion of two lipid bilayers was studied by dynamic force spectroscopy, a value for the distance to the transition state in the order of 10^{-2} nm was obtained by exploiting the Bell-Evans model. This very small value raises problems about its physical meaning. Within the framework of theories about dynamic force spectroscopy, the distance to the transition state expresses the sensitivity of the rate of punch-through to the applied force. A small value of the distance to the transition state means a small sensitivity to the applied force. Nevertheless, the transition state should be able to separate significantly the two equilibrium states of the reaction. A similar problem appears also in the case of force spectroscopy experiments performed to study the unfolding of single proteins, where distances to the transition state in the order of 10^{-1} nm could be obtained. In a recent paper, Best et al. discussed the problem connected with the assumption of the pulling direction as the reaction coordinate for force spectroscopy experiments [10]. Even if this choice is very intuitive, they demonstrated that in many cases, especially for small forces, the pulling direction is not the right choice for the reaction coordinate. In some cases this choice results in the impossibility to separate the folded from the unfolded states due to the transition state being positioned very near to the folded state. It could be possible that a similar situation applies to our case. The pushing direction of the AFM tip probably is not a good reaction coordinate for the process of membrane rupture. In fact, the collapsing event is probably related to the modification of the lateral interactions between the molecules which act perpendicularly to the pushing direction. Further experiments and the consideration of a multidimensional energy landscape could contribute to shedding light on this aspect.

Jump-through force value distributions

Another source of information comes from the distributions of the forces for different tip speeds. Depending on the different model adopted, dissimilar behaviors for the standard deviation of the distributions are predicted. In the manuscript we preferred to consider mainly the most probable jump-through force as a parameter to infer the model from the data. This is due to the fact that bad force curves can substantially affect the distributions whereas the most probable force value is less affected by the presence of bad force curves. However, here we provide examples of the obtained distributions. In figure S8, four examples of distributions of punch-through forces are reported. Figures S8a and 8b represent distributions obtained at 34°C at 760 nm/s and 6500 nm/s tip speeds respectively, whereas the distributions in figures S8c and S8d were obtained at 27°C at 760 nm/s and 6500 nm/s tip speeds respectively. For both temperatures the distributions at low tip speeds have a low-force tail, whereas the distributions for high speeds have tails on the opposite side. A similar result has been obtained by Evans et al. in the case of tension ramps applied to lipid bilayers till rupture [11]. The reason for this behavior has been attributed to the different mechanisms controlling lipid rupture at low and high speed. Interestingly, the standard deviation of the obtained rupture-force values in our data does not raise by increasing the tip speed as it would

be expected for a single bond in the DHS theory. A similar behavior has been foreseen for multiple bonds configured as a zipper [12].

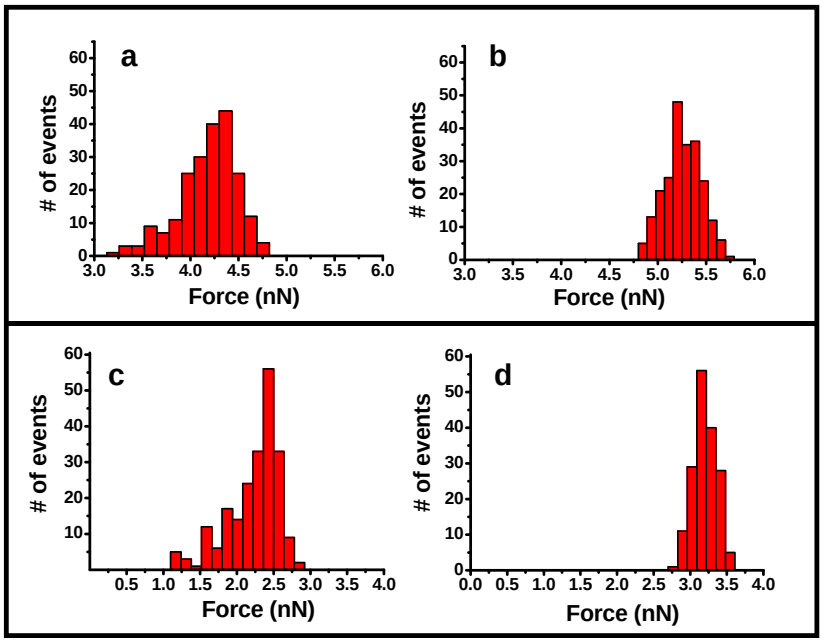

Figure S8: Distribution of the jump-through forces on a coupled supported POPE bilayer. a) 34°C tip-speed 760 nm/s ; b) 34°C tip speed 6500 nm/s; c) 27°C tip speed 760 nm/s; d) 27°C tip speed 6500 nm/s.

Supporting References

[1] Das, C., K.H. Sheikh, … S.D. Connell. 2010. Nanoscale mechanical probing of supported lipid bilayers with atomic force microscopy. *Phys. Rev. E* 82:041920.

[2] Fraxedas, J., S. Garcia-Manyes, … F. Sanz. 2002. Nanoindentation: Toward the sensing of atomic interactions. *Proc. Natl. Acad. Sci. USA* 99:5228-32

[3] Garcia-Manyes, S., G. Oncins, and F. Sanz. 2005. Effect of ion-binding and chemical phospholipid structure on the nanomechanics of lipid bilayers studied by force spectroscopy, *Biophys. J.* 89:1812-26.

[4] Leonenko, Z.V., E. Finot, … D.T. Cramb. 2004. Investigation of temperature-induced phase transitions in DOPC and DPPC phospholipid bilayers using temperature-controlled scanning force microscopy. *Biophys. J.* 86:3783-93.

[5] Cappella, B., and G. Dietler. 1999. Force-distance curves by atomic force microscopy. *Surface Science Reports* 34:1-104.

[6] Picas, L., F. Rico, and S. Scheuring. 2012. Direct measurement of the mechanical properties of lipid phases in supported bilayers. *Biophys. J.*102:L01-3.

[7] Loi, S., G. Sun, … H. J. Butt. 2002. Rupture of molecular thin films observed in atomic force microscopy. II. Experiment. *Phys. Rev. E*, 66:031602.

[8] Sullan, R.M., J.K. Li, … S. Zou. 2010. Cholesterol-dependent nanomechanical stability of phase-segregated multicomponent lipid bilayers. *Biophys. J.* 99:507-16.

[9] Abdulreda, M.H., and V.T. Moy. 2007. Atomic force microscope studies of the fusion of floating lipid bilayers. *Biophys. J.* 92:4369-4378.
[10] Best, R.B., E. Paci, … O.K. Dudko, 2008. Pulling direction as a reaction coordinate for the mechanical unfolding of single molecules. *J. Phys. Chem. B* 112:5968-5976.
[11] Evans, E., V. Heinrich, … W. Rawicz. 2003. Dynamic tension spectroscopy and strength of biomembranes. *Biophys. J.* 85:2342-50.
[12] Williams, P. M. 2003. Analytical descriptions of dynamic force spectroscopy: behaviour of multiple connections *Anal. Chim. Acta*. 479:107-115.